LA-UR- OU - 1817

Title: Nonlinear Feature Identification of Impedance-based
Structural Health Monitoring

Author(s): Amanda C. Rutherford
Gyuhae Park
Hoon Sohn
Charles R. Farrar

•Los Alamos
NATIONAL LABORATORY

Nonlinear Feature Identification of Impedance-based Structural Health Monitoring

Amanda C. Rutherford, Gyuhae Park, Hoon Sohn and Charles R. Farrar
Engineering Sciences and Applications – Weapons Response Group,
Los Alamos National Laboratory, Los Alamos NM, 87545

ABSTRACT

The impedance-based structural health monitoring technique, which utilizes electromechanical coupling properties of piezoelectric materials, has shown feasibility for use in a variety of structural health monitoring applications. Relying on high frequency local excitations (typically>30 kHz), this technique is very sensitive to minor changes in structural integrity in the near field of piezoelectric sensors. Several damage sensitive features have been identified and used coupled with the impedance methods. Most of these methods are, however, limited to linearity assumptions of a structure. This paper presents the use of experimentally identified nonlinear features, combined with impedance methods, for structural health monitoring. Their applicability to damage detection in various frequency ranges is demonstrated using actual impedance signals measured from a portal frame structure. The performance of the nonlinear feature is compared with those of conventional impedance methods. This paper reinforces the utility of nonlinear features in structural health monitoring and suggests that their varying sensitivity in different frequency ranges may be leveraged for certain applications.

Keywords: Structural health monitoring, piezoelectric materials, impedance method, nonlinearity

1. INTRODUCTION

The goal of structural heath monitoring systems is to provide a warning when damage is incipient rather than when serious damage requiring extensive repairs has occurred. Recently, the structural community has turned its attention to developing high-frequency, in-service damage identification techniques that provide required sensitivity to localized, minor defects in the system. Piezoelectric materials (PZT) are particularly useful for this purpose because they can perform both duties of sensing and actuation ("self sensing") within a local area of the structure. One example of documented success using PZTs for self sensing is with impedance-based structural health monitoring methods (Park, 2003).

It is a well-known fact that nonlinear dynamic features of a structure are more sensitive to many common types of damage than linear features. There are many cases where the undamaged structure responds to dynamic loading in a predominantly linear manner and then in a nonlinear manner when the damage is present. Therefore, a combination of the impedance methods with existing nonlinear feature extraction methods is the subject of this paper. The focus of this study is to investigate the performance of nonlinear features, extracted using a frequency domain auto-regressive model with exogenous inputs (ARX) model, from measured impedance signatures. This frequency domain ARX model was originally proposed by Adams (2001). The performance of the nonlinear feature is then compared with those of conventional impedance methods. The varying sensitivity of the extracted nonlinear features in different frequency ranges is also analyzed.

The rest of this paper will involve introduction of the impedance method, experiments conducted on a portal frame structure, extraction of linear and nonlinear features in various frequency ranges, qualitative comparison of features and results.

2. IMPEDANCE METHODS WITH FEATURE EXTRACTION

The impedance-based health monitoring technique has been applied to a wide variety of structures as a promising tool for real-time structural damage assessments (Park et al. 2000; Giurgiutiu et al., 2002; Park et al., 2003). The basic concept of this technique is to monitor the variations in the structural mechanical impedance caused by the presence of damage. Because mechanical impedance measurements can be difficult to obtain, the technique utilizes the electro-mechanical coupling property of PZT. The PZT's electrical impedance is directly related to the mechanical impedance and, hence, will also be affected by the presence of damage. In order to ensure high sensitivity to incipient damage, the electrical impedance is measured at high frequencies (typically greater than 20 kHz), at which the wavelength of the excitation is smaller than the characteristic length of the damage in a structure. A more detailed description of the technique can be found in the references.

2.1. Impedance methods and linear feature extraction

In structural health monitoring, the process of feature extraction is required for the selection of the key information from the measured data that distinguishes between a damaged and an undamaged structure. The extractions also accomplish the condensation of large amount of available data into a much smaller data set that provides concise damage indication. In impedance methods, damage sensitive features are traditionally employed with the use of a scalar damage metric. In earlier work (Park et al 2000), simple statistical algorithm, which is based on frequency-by-frequency comparisons and referred to as 'Root Mean Square Deviation' (RMSD) has been used,

$$M = \sum_{i=1}^{n} \sqrt{\frac{[\mathrm{Re}(Z_{i,1}) - \mathrm{Re}(Z_{i,2})]^2}{[\mathrm{Re}(Z_{i,1})]^2}} \tag{1}$$

where M represents the damage metric, $Z_{i,1}$ is the impedance of the PZT measured at healthy conditions, and $Z_{i,2}$ is the impedance for the comparison with the baseline measurement at frequency interval i. In a RMSD damage metric chart, the greater numerical value of the metric, the larger the difference between the baseline and the impedance measurement of interest indicating the presence of damage in a structure.

Another scalar damage metric, referred to as the 'Cross-Correlation' metric, can also be used to interpret and quantify information from different data sets. The correlation coefficient between two impedance data sets determines the linear relationship between the two signatures

$$\rho = \frac{1}{n-1} \frac{\sum_{i=1}^{n}(\mathrm{Re}(Z_{i,1}) - \mathrm{Re}(\overline{Z}_1))(\mathrm{Re}(Z_{i,2}) - \mathrm{Re}(\overline{Z}_2))}{s_{Z_1} s_{Z_2}} \tag{2}$$

where ρ is the correlation coefficient, $Z_{i,1}$ and $Z_{i,2}$ are as described above, $\overline{Z}_1$ and $\overline{Z}_2$ are the means of the signals and the s terms are the standard deviations. For convenience, the feature examined in this case is typically $(1-\rho)$; this is done merely to ensure that with increasing damage or change in structural integrity, the metric values also increase. This provides an aesthetic metric chart and is consistent with other metrics, such as RMSD, in which metric values increase when there is an increase in damage. The cross-correlation metric account for vertical and horizontal shift of entire impedance signature, usually associated with temperature changes. In most cases, the results with the correlation metric are consistent with those of RMSD. Zagrai and Giurgiutiu (2001) investigate several statistics-based damage metrics, including RMSD, mean absolute percentage deviation, covariance change, and correlation coefficient deviation. It has been found that the third power of the correlation coefficient deviation, $(1-\rho)^3$, is the most successful damage indicator, which tends to linearly decrease as the crack in a thin plate moves away from the sensor.

2.2. Impedance methods and nonlinear feature extraction

The linear features described above are well suited to situations in which one structural state is to be discriminated from another in a linear sense, but they would not be able to quantify any nonlinear changes. Because the frequency ranges of

impedance measurements are typically high, it is hypothesized that some structural nonlinearities will be captured in the measurement. A nonlinearity in a structure could manifest itself in an impedance signal in a few different ways. Nonlinearities often result in changes in amplitude, peak shifts, and peak shape changes. Nonlinearity in a structure can result in changes in the impedance signature with changing input force levels. Nonlinearities may also result in frequency response that is correlated to both the input and the output at various frequencies (Adams et al., 2004).

Some very simple features that have been utilized by Rutherford et al (2004) are impedance moments. In their study, the concept of "moment" is applied as additional single number features resulting from the following formulation,

$$M_i = \int_{-\infty}^{\infty} \omega^i f(\omega)^2 d\omega \tag{3}$$

where M_i is the ith moment, ω is the frequency in this case, and $f(\omega)$ is the impedance signal. The zeroth moment may be thought of as the energy in the impedance signal (capturing changes in peak amplitude and shape). The first moment is the "centroid" of the signal, or it divides the signal into two equal energy bandwidths. The second moment is the RMS duration of the signal. In standard formulation, moments are normalized by the zeroth moment and zero through second normalized moments are referred to as E, T, and D respectively.

Additional features that have been examined are coefficients of an ARX model of the impedance signal. This method, presented by Adams (2001), has been applied by Fasel et al. (2003). An ARX model in the frequency domain accounts for the "feedback" that may occur between inputs and outputs in a nonlinear structure. It does so with the following formulation,

$$\mathbf{Y}(k) = \mathbf{B}(k)\mathbf{U}(k) + \mathbf{A}_x(k)\mathbf{Y}(k-1) + \mathbf{A}_{-x}(k)\mathbf{Y}(k+1) \tag{4}$$

where $\mathbf{Y}(k)$ is the output, $\mathbf{U}(k)$ is the input signal, k is the kth frequency and x is the size of the window. $\mathbf{A}_x(k)$ and $\mathbf{A}_{-x}(k)$ are the autoregressive (nonlinear) coefficients. $\mathbf{B}(k)$ is the exogenous (linear) coefficient. Because in the case of impedance signals, $\mathbf{Y}(k)$ and $\mathbf{U}(k)$ are complex numbers, the coefficients are also complex, meaning that six values must be determined. The way this is accomplished is by windowing the available data into more blocks than coefficients and then minimizing the squared error between the prediction and the measured impedance (See Adams 2001; Fasel et al, 2003, for more details).

The work presented in this paper is the extension of the investigation performed by Fasel et al, (2003). The nonlinear features associated with the electro-mechanical impedance measurements are extracted using the frequency domain ARX model. The performance of the nonlinear feature is compared with those of conventional impedance methods. Their varying sensitivity in different frequency ranges is also analyzed. The traditional feature extraction measure of cross-correlation coefficients is calculated and used to compare to those features.

3. TESTING THE PORTAL FRAME STRUCTURE

The structure examined in this work was a simple moment-resisting, portal-frame structure, shown in Figure 1 below. The structure consists of aluminum members connected using steel angle brackets and screws, with a simulated rigid base. The beam is 0.25 in thick, 2.00 in wide and 22.00 in long. The two columns are 0.25 in thick, 2.00 in wide and 12.00 in tall. The base is 0.50 in thick, 6.00 in wide and 24 in long. The steel angle brackets are 0.25 in thick, 2.00 in wide and 2.50 in long. Bolts were torqued to 150 in-lbs in the healthy condition. PZTs (1.00 in x 1.00in x 0.01in) were mounted on the left side of the symmetric structure (Corner 2), with PZT 1 mounted on the column and PZT 2 mounted on the beam, as shown in Figure 2.

In this study, the voltage into the PZT is used as the output to the frequency domain ARX model and the voltage output from the PZT circuit, as seen in Figure 3, is used as the input. These voltages are measured in the time domain, which is different from the traditional impedance-based methods that only record data in the frequency domain. V_{out} is proportional to the output current of the PZT. Electrical impedance of the PZT patch is related to the measured input and output voltage of the PZT through the following equation:

$$Z_p = \frac{V_p}{I_p} = \frac{V_{in} - V_{out}}{V_{out}/R} \quad \Rightarrow \quad Z_p = R\left(\frac{V_{in}}{V_{out}} - 1\right) \qquad (5)$$

A commercial data acquisition system controlled from a laptop PC is used to digitize the voltage analog signals. For the nonlinearity analysis, time histories were sampled at a rate of 51.2 kHz, producing 32,768 time points. The frequency domain ARX method requires data to be recorded in the time domain, and current hardware limitations only allow time domain data to measure under that sampling frequency. In addition, a total of 20 averages per run, under the same configuration, were used for traditional impedance estimates in the frequency domain. An amplified random signal (2.5 V) was used as the voltage input for both testing.

Baseline measurements of a structure should seek to capture all types of variability that the structure might be subject to, which would not be attributed to damage, such as environmental effects. Previous experimentation on this portal frame structure performed by Aumann et al, (2003) revealed that variability in the portal frame due to assembly and disassembly is also significant. Baseline measurements in this set of experiments set out to capture, to some extent, typical environmental variability and assembly/disassembly variability (by disassembling the top beam). A total of 6 baseline time histories were recorded for both PZTs, with conditions noted in Table 1 below. Two damage states were then introduced at two different locations by loosening the bolts at those locations to 75 ft-lbs and then hand tightening. After implementing the damage, the time histories were again recorded from each PZT. The full test matrix is shown below in Table 1.
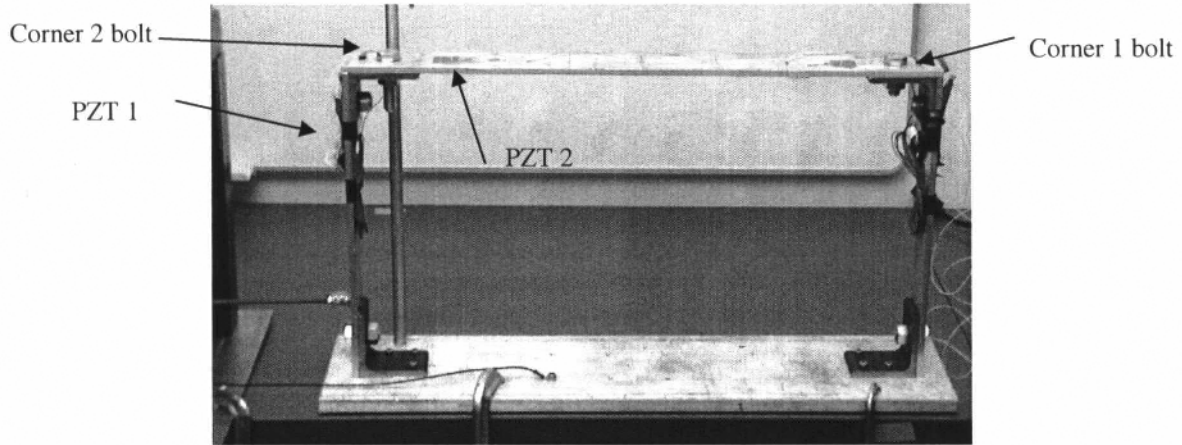

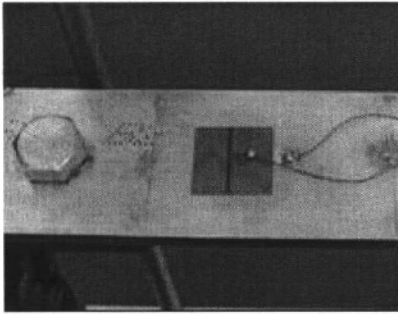Figure 1: The portal frame structure tested (actual data acquisition used not shown).
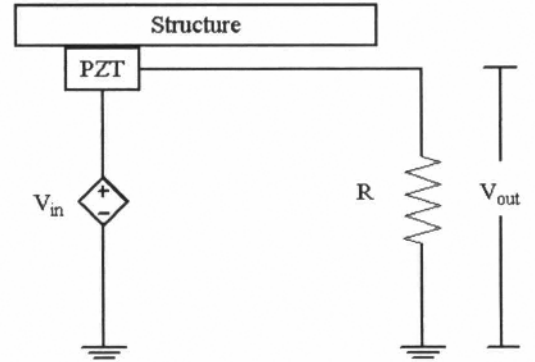

Figure 2: PZT 2 installed on the top beam

Figure 3: Diagram of PZT circuit indicating locations of measured voltages V_{in} and V_{out}

Table 1: Test Matrix for the Portal Frame Structure	
Test 1	Baseline: Undamaged
Test 2	Baseline: No change from Test 1, take measurement two hours later
Test 3	Baseline: Disassemble/reassemble the top beam; take measurement
Test 4	Baseline: Disassemble/reassemble the top beam; take measurement
Test 5	Baseline: No change from Test 4, take measurement after 12 hours
Test 6	Baseline: Disassemble/reassemble the top beam; take measurement
Test 7	D11: Loosen corner 1 bolt to 75 in-lb
Test 8	D12: Hand tighten corner 1 bolt
Test 9	Baseline: Retighten to 150 in-lb
Test 10	D21: Loosen corner 2 bolt to 75 in-lb
Test 11	D22: Hand tighten corner 2 bolt

The baseline impedance measurements are shown below in Figures 4 and 5 in the frequency range of 10-20 kHz. For PZT 1, even after the assembly/disassembly procedure, the impedance signatures are repeatable and show relatively small changes. The variation is anticipated to increase in PZT 2 because PZT 2 is installed directly into the top-beam (the component that is disassembled and reassembled). Large baseline variations in PZT 2 can be observed in Figure 5. The variation in the signal due to damage needs to be greater than the baseline variations in order to be detectable. Figure 6 illustrates PZT 1's baselines and signals measured after the damage at Corner 1 (D11, D12 in Table 1). Figure 7 shows baselines and damaged signals that introduced at Corner 2 (D21, D22 in Table 2) from PZT 2. It is easy to see that qualitatively that damaged signals are quite different with the appearance of new peaks and shifts of old ones, especially at the higher frequency levels. With increasing levels of the damage, the impedance variation becomes also more noticeable. The other results, i.e. PZT 1 for D21, D22 and PZT 2 for D11, D12, are similar. The size of the structure and relatively low impedance frequency range (10-20 kHz) employed limits the ability of the PZTs to detect damage "locally". Both PZTs show some sensitivity to damage at Corner 1 and Corner 2. The impedance frequency must be kept higher in order for the damage to be localized, because then the PZTs are sensitive to the damage in the near field and less sensitive to changes in far-field.
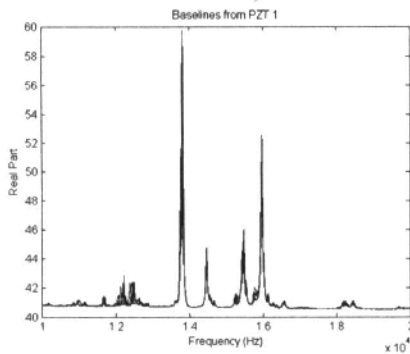

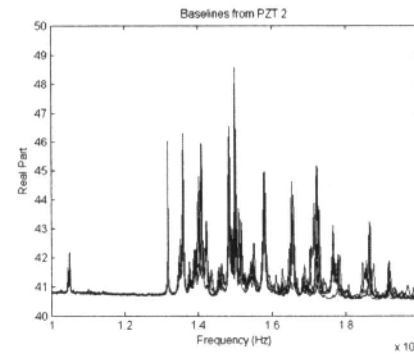Figure 4: Baselines of PZT 1, 6 measurements are shown w/o label.

Figure 5: Baselines of PZT 2. A relatively large variations was observed compared to PZT 1.
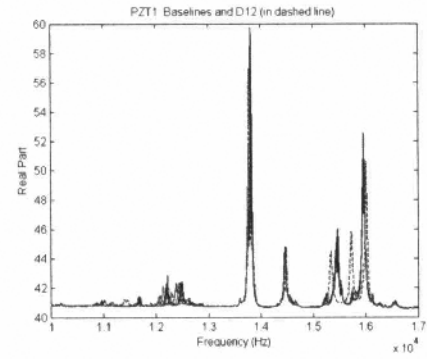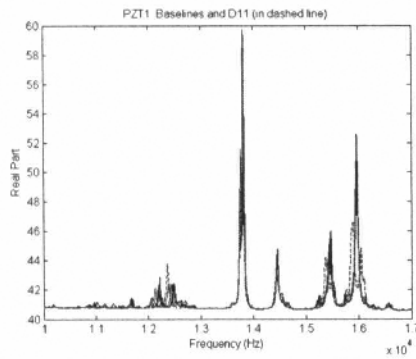
Figure 6. PZT 1, baselines and damage at corner 1; D11: 75 in-lb and D12: hand tightened.
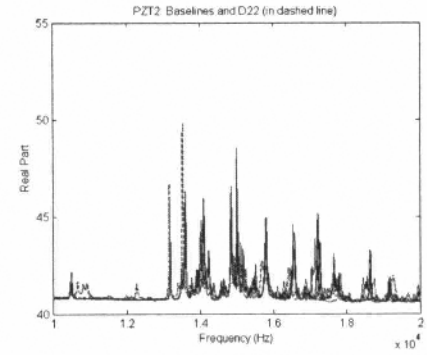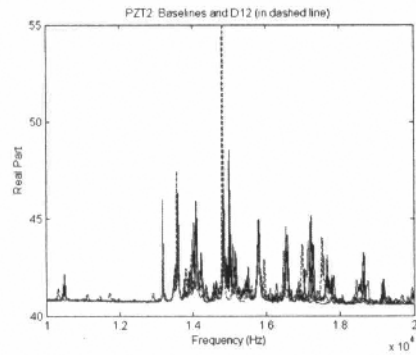

Figure 7. PZT 2, baselines and damage at corner 2; D21: 75 in-lb and D22: hand tightened.

Quantification of damage was the next step taken. Cross-correlation coefficients are calculated and used to assess the conditions of the structure. Cross correlations were calculated between six baseline measurements and each tested case. The first baseline is used as a "true" undamaged signature, which all other measurement are compared to. Results for PZT 1 and PZT 2 are shown in Figures 8 and 9 below. Cross correlations confirm what was suspected upon initial observation of the signals. The frequency employed and size of the structure limits the ability of the PZTs to detect damage locally at Corner 1. However, the cross correlation of PZT 1 reveals that it may distinguish between the 75 in-lb case and the hand tightened damage cases. The extent and distance of damage is somewhat related to the coefficients values. The cross correlation of PZT 2 does not show the same characteristics. It shows relatively large variations compared to PZT1 and it is only able to distinguish between damaged and undamaged states of the portal frame. This could be because of the close proximity of PZT2 to both of the damaged joints and its location on the top beam that is being assembled and disassembled.
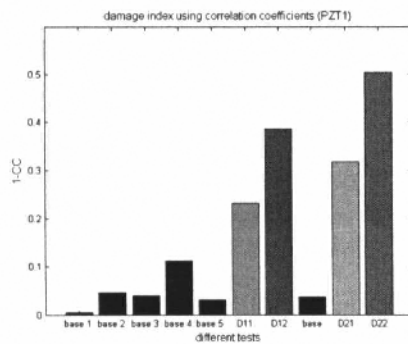

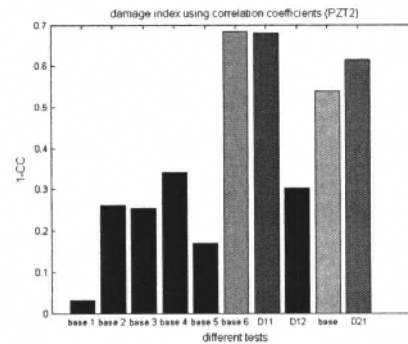Figure 8 Cross Correlation Damage Metric Chart of PZT 1

Figure 9. Cross Correlation Damage Metric Chart of PZT 2

4. NONLINEAR FEATURE EXTRACTION FROM IMPEDANCE DATA

Quantification of the differences between the baselines and the damage cases through application of linear and nonlinear feature extraction methods is the subject of this section. Linear and nonlinear features were extracted in the form ARX model coefficients. While the structure exhibits global linearity, it was hypothesized that nonlinearities would be present in the data due to the contacting interfaces of the parts, and differences in these interfaces introduced in assembly/disassembly of the top beam. Once again, correlation coefficients are calculated and used to compare the calculated ARX coefficients.

First, all time history data are first normalized by subtracting the mean and dividing by the standard deviation, as in the following equation,

$$\overline{\mathbf{x}} = \frac{\mathbf{x} - \mu}{\sigma} \tag{6}$$

where $\mathbf{x}$ is the original vector, $\overline{\mathbf{x}}$ is the normalized vector, μ is the mean of the original vector and σ is the standard deviation of the original vector. This process is used so that the damage detection algorithm can distinguish between structural damage and operational variability (Sohn et al 2000).

In order to establish the ARX coefficients, multiple sets of data need to be available while the structure is in the same condition. Because only one 32,768-point time history is available for each condition, each time history is split up into 29 separate 4096-point blocks with 75% overlap. At this point, a Hanning window is applied to each block of data. A Fast Fourier Transform (FFT) is then performed on all data blocks in order to transfer the time history information into the frequency domain. There are 29 equations (from the 29 FFTs) and 6 unknown coefficients, for each frequency value k, that must be solved. $\mathbf{B}(k)$, $\mathbf{A}_1(k)$ and $\mathbf{A}_{-1}(k)$ in equation (4) are then determined by minimizing the sum of the squared error associated with how well the ARX model in equation (4) describes the measured impedance data.

The real parts of the linear coefficients are plotted in Figures 9, and the magnitudes of nonlinear coefficients are shown in Figure 10 for the six baselines of PZT 1. It should be noted that, in the impedance methods, only the real part is usually used for monitoring structures because it is more sensitive to structural damage than the imaginary part (Park et al. 2003). Therefore, for the frequency ARX model, only the real part is used for the analysis. The linear coefficients look very similar to the actual impedance signals plotted in Figure 4. Figures 12 and 13 show the baselines superimposed with the damage case (D22) for nonlinear coefficients of both PZTs, in the higher frequency range, where distinct variations occur. The changes in the linear features with induced damage follow essentially the same pattern as in the cases of impedance signatures, as already illustrated in Figures 6 and 7.
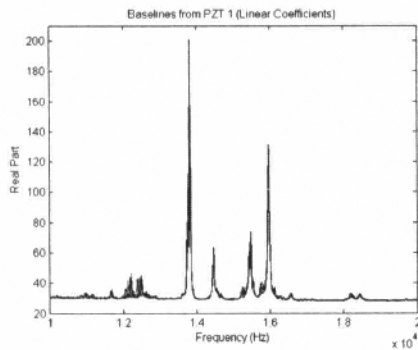

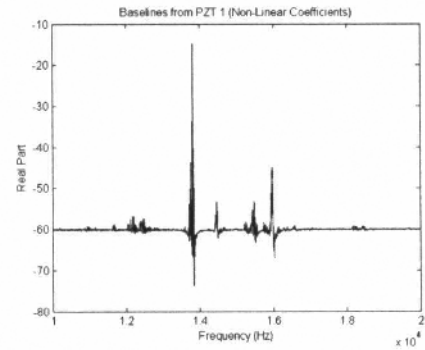Figure 10: Linear coefficients from PZT 1, baselines   Figure 11: Nonlinear coefficients from PZT 1, baselines
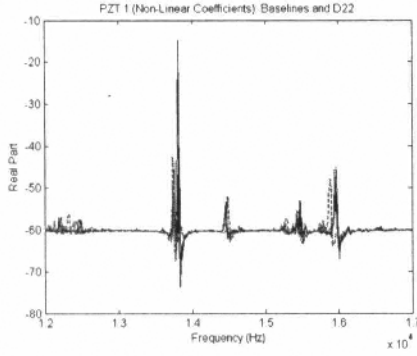
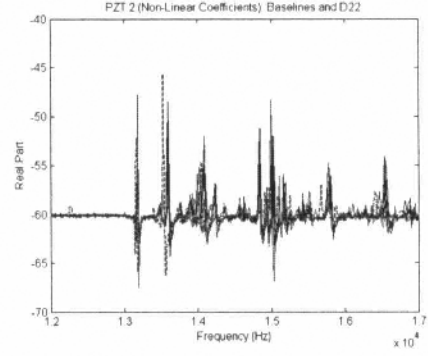Figure 12: Nonlinear coefficients from PZT 1, baselines and D22

Figure 13: Nonlinear coefficients from PZT 2, baselines and D22

From the figures it is apparent that the damaged signatures differ from the undamaged cases significantly. In order to quantify this difference, a cross correlation was calculated for the ARX coefficients. That is, the cross correlation between each of the tests and the first baseline set of coefficients was calculated. Because of the similarity between the linear coefficients and the original impedance signals, cross correlations of these coefficients yielded results that were very similar to cross correlation of the impedance signals. The variations associated with the rebuilding procedure is somewhat reduced compared to original signals, however, the sensitivity to presence of damage is also reduced.

Analysis of the nonlinear coefficients yielded some interesting results, as shown in Figures 14-15. The variations of baselines are relatively large compared to those of the original impedance signals or linear coefficients. Because of relatively larger variations, the first damage (D11) could not be definitely identified by PZT 1. On the other hand, the nonlinear coefficients of PZT 1 are somewhat over-sensitive to the presence of other damage cases (D12, D21, D22). For PZT 2, because of the direct contact with the top beam and the damaged joint, baseline variations are much larger and damaged cases are not definitely identified.
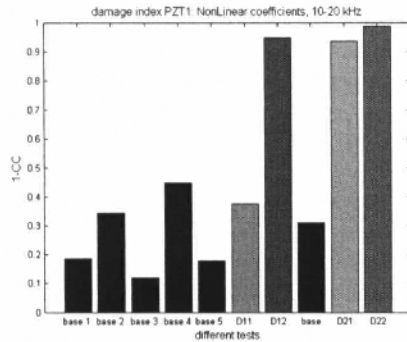

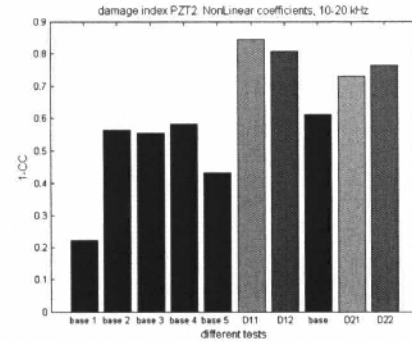Figure 14: Correlation of Non linear coefficients, PZT 1, 10-20 kHz

Figure 15: Correlation of Nonlinear coefficients, PZT 2, 10-20 kHz

It can be concluded from the above figures that the nonlinear coefficients might be too sensitive at higher frequency ranges. The linear coefficients, which are close to those shown in Figures 8 and 9, seem to provide a better characterization regarding the conditions of the structure. The next step of this investigation is to examine the sensitivity of nonlinear coefficients at different frequency ranges. For this purpose, frequency response functions (FRF) between PZT 1 and PZT 2, instead of electrical impedances, were used. This is because the low frequency ranges of electrical impedance are dominated by the capacitive nature of the piezoelectric materials, making it difficult to obtain structural impedance data in low frequency ranges. The same experimental and analytical procedures are used as with the impedance method. As can be seen in equation (5), the imaginary part of FRF is analogous to the real part of the electrical impedance (linear coefficients). Therefore, only the imaginary parts are examined are examined. Figure 16 shows the imaginary part of the linear and nonlinear coefficients of the FRF between PZT1 and PZT2 with induced damage (D12)
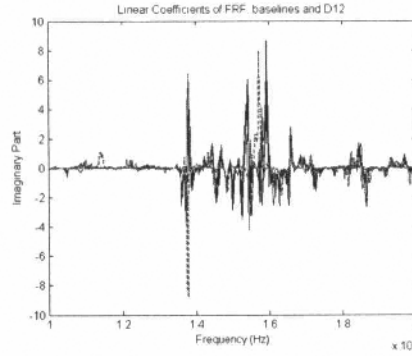
Figure 16: Linear coefficients from FRF between PZT1 and PZT2, baselines and D12

The correlations were examined for linear and nonlinear coefficients at two different frequency bands, 0-2 kHz and 15-23 kHz as shown in Figures 17 and 18. At lower frequency ranges, the linear coefficients could not definitively identify the small-scale damage cases (torque reduced to 75 in-lbs), but the nonlinear coefficients could. In this case, the nonlinear features increased sensitivity makes it superior to the linear features at lower frequency ranges, as confirmed by numerous studies. At higher frequency ranges, however, the nonlinear feature seems to be somewhat over-sensitive to baseline variation and presence of damage is not as clear. On the other hand, the linear feature has much more baseline repeatability and hence it can discriminate between baselines and damage cases. These observations from FRF data confirm what has been observed in previous studies combining nonlinear features and impedance sensing. Based on these results, the nonlinear coefficients of the impedance data were once again analyzed, but this time in just the lower frequency ranges (1-4 kHz). All damage cases could be successfully identified as shown in Figures 19-20.
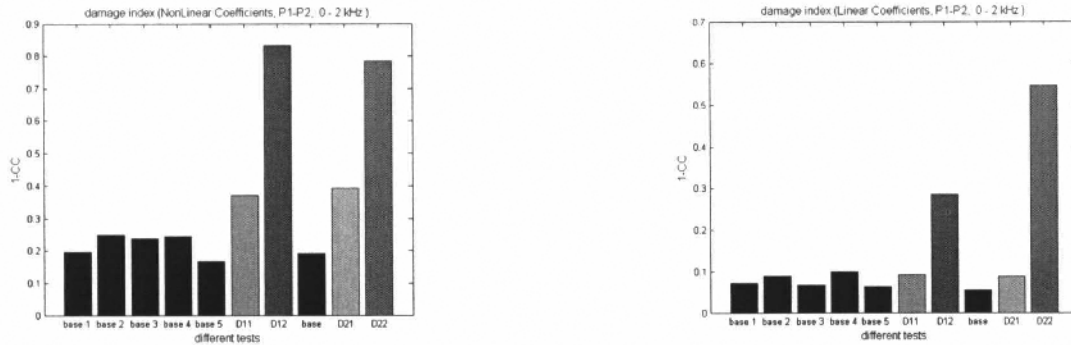

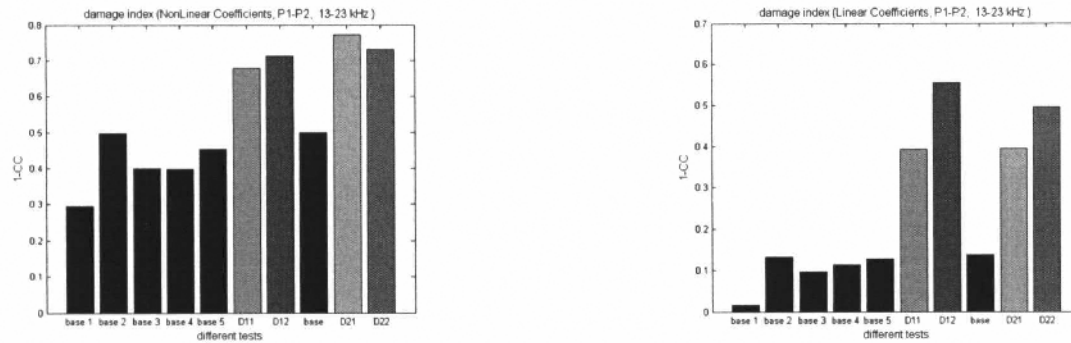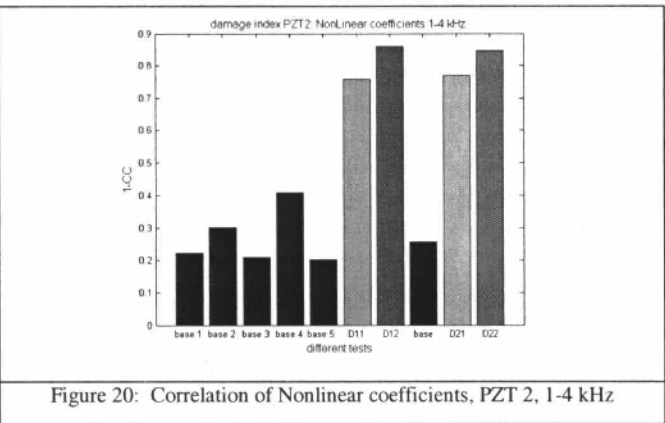Figure 17: Correlation of Nonlinear and linear coefficients, PZT 1-2 FRF, 0-2 kHz

Figure 18: Correlation of Nonlinear and linear coefficients, PZT 1-2 FRF , 15-23 kHz

It can be concluded from these observations that nonlinear features, in the form of nonlinear ARX model coefficients, demonstrated varying sensitivity to damage depending on the frequency range examined with increased sensitivity (to all types of variability) at higher frequency ranges. Some other nonlinear features, including reciprocity checks, changes in

the magnitude of applied force (FRF distortions), and time-domain AR-ARX models, show the same kind of characteristics. This quality of nonlinear features could be leveraged in several ways. First, a signal processing technique that could capitalize on the increased sensitivity could better characterize structural conditions. In this study, we only examined cross-correlation coefficients to assess the performance of the nonlinear feature (and the RMSD shows similar results). Other statistical feature extraction methods could be used in concert with the ARX nonlinear coefficients (such as moments, variance normalized coefficients, etc.) to improve sensitivity to damage by potentially decreasing baseline variability. Another desirable quality of the low frequency range sensitivity of the nonlinear coefficients is that hardware sampling and data storage requirements could be relaxed. The changing sensitivity of nonlinear features with frequency range could be leveraged for sensor locations that are not ideal; *ie*, sensors that are far field from damage could have increased sensitivity by looking at nonlinear coefficients for the higher frequency ranges. Finally, the nonlinear feature, especially in the form of the frequency domain ARX model, could be used to enhance the repeatability of the linear features. By removing nonlinear features from frequency responses or impedance estimates, the variations associated with nonlinear uncertainty and sensitivity could be reduced because structural responses at high frequency ranges are usually contaminated by nonlinear variability. The could result in better performance of "filtered" linear features for structural health monitoring.

| Figure 19: Correlation of Non linear coefficients, PZT 1, 1-4 kHz | Figure 20: Correlation of Nonlinear coefficients, PZT 2, 1-4 kHz |
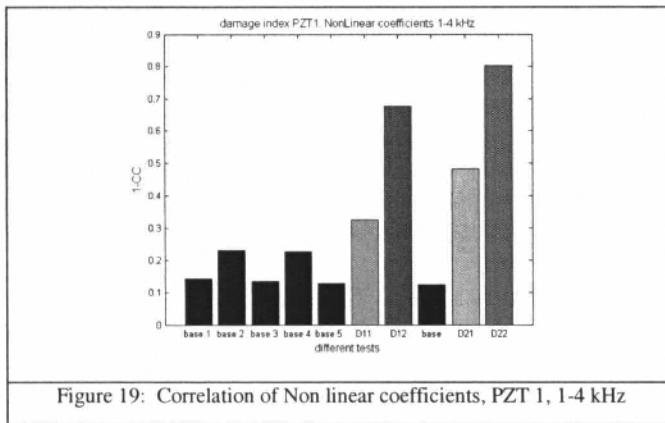
5. CONCLUSIONS

Both linear and nonlinear features of piezoelectric impedance are analyzed for structural health monitoring applications. A series of experiments was performed on a portal frame. The linear shows an excellent capability at higher frequency ranges. Nonlinear features, in the form of nonlinear ARX model coefficients, demonstrated varying sensitivity to damage depending on the frequency range examined, with increased sensitivity (to all types of variability) at higher frequency ranges. This work further reinforces the utility of the use of nonlinear features for damage identification. Future work will include more investigation into binning of frequency ranges when using ARX coefficients, changing window size when fitting ARX models, looking at additional statistical feature extraction methods and testing of more complex structures.

ACKNOWLEDGMENTS

REFERENCES

1. Adams, D.E., "Frequency Domain ARX Models and Multi-Harmonic FRF Estimators for Nonlinear Dynamic Systems," *Journal of Sound and Vibration,* :Vol. 250, No. 5, pp. 935-950, 2001.
2. Aumann, R.J., McCarty, A.S., and Olson, C.C., "Identification of Random Variation in Structures and Their Parameter Estimates," Proceedings of the 22nd IMAC, Kissimee, FL, 2003.
3. Fasel, T.R., Sohn, H., Park, G., and Farrar, C.R., "Application of Frequency Domain ARX Models and Extreme Value Statistics to Impedance Based Damage Detection," Proceedings of IMECE 2003, Washington, D.C.

4. Giurgiutiu, V., Zagrai, A., Bao, J.J., "Piezoelectric Wafer Embedded Active Sensors for Aging Aircraft Structural Health Monitoring," *International Journal of Structural Health Monitoring,* Vol. 1, pp. 41-61, 2002.

5. Park, G., Cudney, H., Inman, D.J., "Impedance-based Health Monitoring of Civil Structural Components," *ASCE Journal of Infrastructure Systems,* Vol. 6, No. 4, pp. 153-160, 2000.

6. Park, G., Sohn, H., Farrar, C.R., Inman, D.J., "Overview of Piezoelectric Impedance-based Health Monitoring and Path Forward," *The Shock and Vibration Digest,* Vol. 35, No.6, 2003.

7. Rutherford, A.C., Park, G., Sohn, H., and Farrar, C.R., "The Use of Electrical Impedance Moments for Structural Health Monitoring," Proceedings of the 22nd IMAC, Dearborn, MI, 2004.

8. Sun, F.P., Chaudhry Z., Liang, C. and Rogers C.A., "Truss Structure Integrity Identification Using PZT Sensor-Actuator," *Journal of Intelligent Material Systems and Structures,* 6, 134-139, 1995.

9. Zagrai, A.N. and Giurgiutiu,V., "Electro-Mechanical Impedance Method for Crack Detection in Thin Plates," *Journal of Intelligent Material Systems and Structures,* 12, 709-718, 2001.

10. Sohn H, Czarnecki JJ, Farrar CR. Structural Health Monitoring Using Statistical Process Control. *Journal of Structural Engineering* 2000; **126**(11):1356-1363.